Evaluation of Seismic Performance of Wooden Houses during the Northern Miyagi Earthquakes of July 26, 2003

Hidemaru SHIMIZU*, Yasuhiro HAYASHI**, Yoshiyuki SUZUKI***,
Takeshi MORII**** and Kyousuke MUKAIBOU****

* COE Researcher, DPRI, Kyoto University
** Associate Professor, DPRI Kyoto University
*** Professor, DPRI Kyoto University
**** Graduate School of Engineering, Kyoto University

Synopsis

This paper presents the results of our investigation on wooden house damages during the earthquakes in Northern Miyagi, Japan. First, earthquake observation records are summarized. Next, the peak ground velocities in the area of severe damages are estimated from the toppling ratios or displacements of tombstones. Then, from a survey of the damages in three towns, it is found that the damage ratio of one-story houses is much higher than that of two-story houses. This damage trend is analyzed and explained by using the method of equivalent-performance response spectrum. Finally, seismic performances of 21 typical houses are compared based on the response limit strength design method.

Keywords: Northern Miyagi earthquakes, traditional wooden houses, peak ground velocity, damage, height of hanging wall, response limit strength design method

1. Introduction

The Northern Miyagi earthquakes occurred on July 26, 2003 in the Miyagi Prefecture, northern Japan, as shown in Fig. 1. The main shock of the earthquakes occurred at 7:13 AM with magnitude M6.2. The epicenter is located at latitude N38.402, longitude E141.175, with focal depth 12km. The foreshock and the biggest aftershock occurred at 0:13 and 16:56 in the same day, respectively. Very high JMA intensities of more than 6- were observed at many stations during three earthquakes, and thousands of buildings were severely damaged. Especially, the earthquakes caused collapses of many wooden houses. The objective of this paper is to evaluate seismic performances of the wooden houses in the areas with most severe damages.

2. Earthquake observation record

Due to the strong-motion networks developed very densely in this area, a large number of ground motion recordings were acquired. Many records were obtained by local town offices. But only the JMA seismic intensities and peak ground accelerations were printed out, and most of the digital data were lost unfortunately because of being overwritten by many aftershock data.

Fig. 1(a) shows the peak ground velocity (PGV) distributions calculated using accelerograms obtained at the K-NET, KiK-net, and JMA stations during the main shock. A solid line indicates an active fault called as "Asahiyama flexure", which has
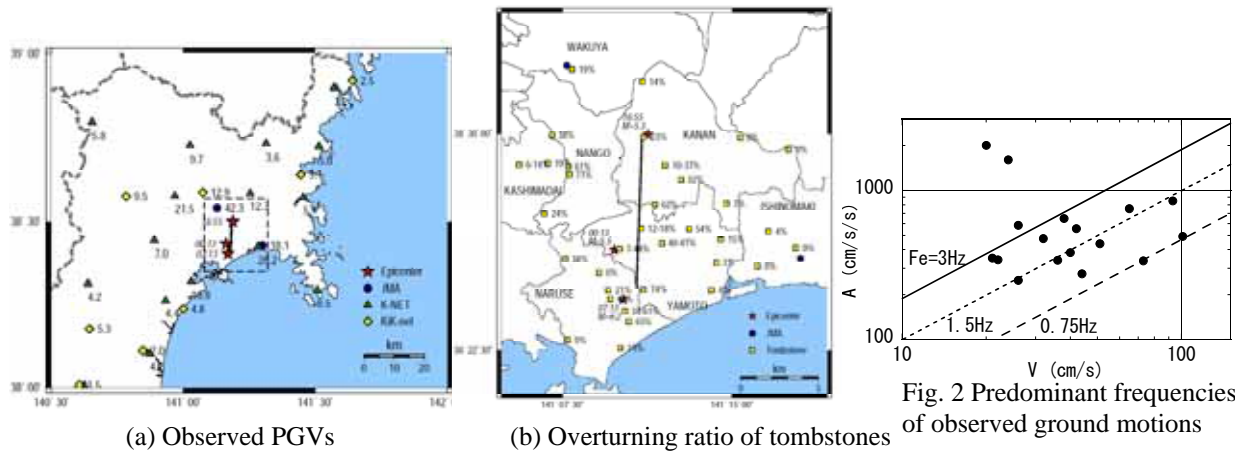
(a) Observed PGVs

(b) Overturning ratio of tombstones

Fig. 1 Observed PGV distribution and overturning ratio distribution of tombstones

Fig. 2 Predominant frequencies of observed ground motions

Table 1 Representative earthquake recordings obtained from three earthquakes

Time	JMA magnitude M_{JMA}	Town	Organization	JMA seismic intensity I_{JMA}	Peak Ground Acc. A (cm/s²)	Peak Ground Vel. V (cm/s)	Epicentral distance (km)	Predominant freq. of soil Fg (Hz)	Predominant freq. of ground motions Fe (Hz)
0:13	5.5	Naruse	Town office	5.9	2005	20	3.5	3.8	16.0
		Yamoto	Town office	5.5	476	32	4.5	2.6	2.4
		Naruse	NILIM	-	440	51	2.6		1.4
7:13	6.2	Yamoto	Town office	6.2	850	93	4.2	2.6	1.5
		Nango	Town office	6.0	491	101	9.9	1.1	0.8
		Naruse	Town office	6.0	756	65	1.0	3.8	1.9
		Kashimadai	Town office	5.9	1606	24	10.5	3.6	10.6
		Wakuya	JMA	5.8	555	42	15.2	0.9	2.1
		Kanan	Town office	5.7	337	73	11.3	1.1	0.7
		Kogota	Town office	5.5	585	26	17.5		3.6
		Momoo	Town office	5.5	383	40	19.7		1.5
		Matsuyama	Town office	5.4	340	36	16.0		1.5
		Ishinomaki	NILIM	-	250	26	11.1		1.5
16:56	5.4	Kanan	Town office	5.7	649	38	1.1	1.1	2.7
		Nango	Town office	5.4	276	44	4.9	1.1	1.0
		Wakuya	JMA	5.2	342	22	6.9	0.9	2.5
		Wakuya	NILIM	-	351	21	6.6		2.7

NILIM V=SI   Town office $I_{JMA}=1.40+0.98\log(AV)$ $Fe=A/V/2\pi$

North-South strike as shown in Fig. 1. Three star marks show the epicenter positions of the foreshock, main shock, and the biggest aftershock, respectively.

The records with PGVs higher than 15 cm/s were observed in the Wakuya station and Ishinomaki station deployed by the JMA. These two JMA stations are 15km and 11km away from the epicenter of the main shock, respectively. Predominant period ranges from 0.3 to 0.6 sec at the Wakuya station and is less than 0.3 sec at the Ishinomaki station.

Table 1 shows representative records obtained from three earthquakes. Relationship between the peak ground accelerations (PGAs) and PGVs is shown in Fig. 2. An extremely high PGA (2005 cm/s²) was recorded in the foreshock event at the NARUSE town office station 3.5km away from the epicenter. A very high PGA (1606 cm/s²) was also obtained in the main shock event at the Kashimadai town office station 10.5km away from the epicenter. Excluding these two records, the predominant frequency Fe at most stations ranges from 0.75 Hz to 3.0Hz as shown in Fig. 2. The estimated PGV reaches about 100 cm/s at the Nango town office station and about 90 cm/s at the Yamoto town office station. However, some of these

values might be affected by amplification effects of surface soils. The predominant frequencies Fg of the soils around the seismic observation stations are also listed in Table 1. The predominant frequency Fg is estimated as the peak frequency of H/V spectrum obtained from the microtremor measurements. The Fg is about 1.1Hz at the Nango town office and the Kanan town office where the Fe's are small. Therefore, the smallness of Fe is due to the soft surface soil condition. In other locations where the soils are not soft, the predominant frequencies are estimated to be greater than 1.5Hz.

3. Outline of investigation

Since the areas with most severe damages of wooden houses are near the epicenters where the number of observation stations is very limited, we were unable to obtain the ground motion intensities directly in these areas. Therefore, preliminary investigation was conducted on July 28 and 29 to evaluate the peak ground velocity distribution in term of the overturning ratio of tombstones in these areas. From August 9 to 12, we performed detailed
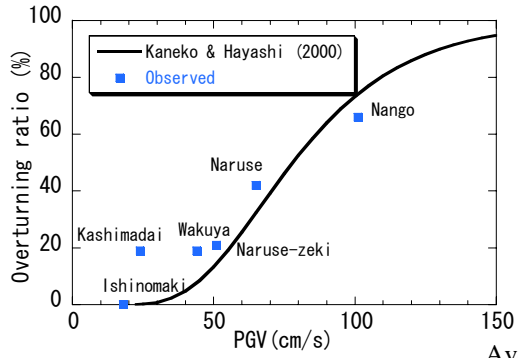
Fig.3 Relation of PGV and overturning ratio of tombstones
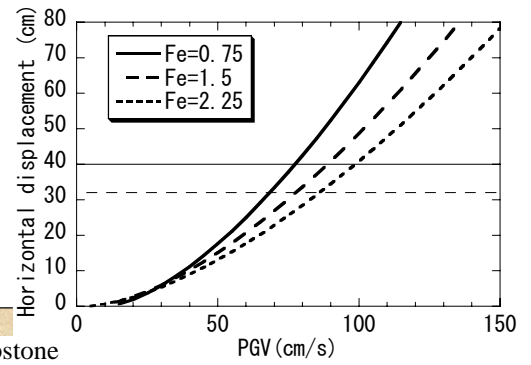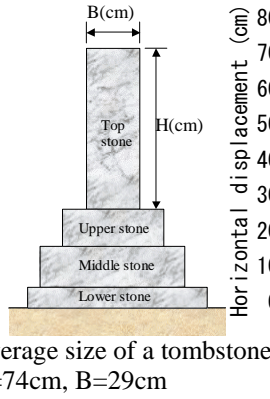
Average size of a tombstone
H=74cm, B=29cm

Fig.4 Relation of PGV and horizontal displacement of tombstones

investigation to grasp structural features and damage characteristics, including microtremor measurements of soils and buildings and simplified surveys to obtain damage statistics. The overturning ratios of tombstones were investigated at 34 sites where marked by □ as shown in Fig. 1(b). The investigated wooden houses are in the Yamoto town, Kanan town, and Nango town, located in the area bordered by dashed lines in Fig. 1(a) and zoomed in as Fig. 1(b).

4. PGV estimated from toppling of tombstones

The observed overturning ratio of tombstones in an area may be used to estimate the PGV of the area. Kaneko and Hayashi (2000) developed the following relation

$$P = \Phi(\{\ln(V) - \ln(V_0)\}/0.4) \qquad (1)$$

where F is the standard normal distribution function, P and V denote the overturning ratio and the PGV, respectively, and $V_0 = 10(B/H^{0.5})(1+B/H)^{2.5}$. Here B and H are the width and height of the top stone of a tombstone, respectively (see Fig. 3). Eq. (1) shows that the overturning ratio of tombstones is affected by the shape and size of the rigid top stones, and slender tombstones (small B/H) tend to topple down easily. In this study, B and H are assumed to be 29cm and 74cm, respectively, according to the average size of the measured tombstones. The relationship (1) between the PGV and the overturning ratio P is shown by a solid line in Fig. 3. Also depicted in the figure by solid square marks is the relationship of the maximum PGV value during three earthquakes at a seismic observation station listed in Table 1 and the overturning ratio of tombstones at the nearest grave to the station. The two relationships show good agreement as seen in Fig. 3. Therefore, we can estimate the PGV in terms of the overturning ratio in the same area. Consequently, in the areas with severe damages near the Asahiyama flexure, the PGVs are estimated to be 85 to 100cm/s according to the overturning ratios of 60-75%.

However, Eq. (1) is not applicable to those tombstones which have been strengthened using dowels to connect the top, upper, and lower stones together to prevent it from toppling. The dowels are made of steel bars or cylindrical stones. In these cases, the tombstones slide during earthquakes and may finally fall down. Fig. 3 shows a tombstone that slid and fell down during the Northern Miyagi earthquakes. It is interesting that the material of the top and upper stones was different from that of the middle and lower stones. Probably, this tombstone was damaged during the Miyagi-Oki earthquake in 1978, and reinforced by using doweling.

The widths of the lower stone and middle stone are about 80 cm and 64 cm, respectively. Therefore, in order for the jointed tombstone to fall down, it is necessary for the lower part to slide more than half-width (40cm or 32cm). The PGV required to make the jointed part to fall down can be estimated by using the following formula developed by Kaneko & Hayashi (1999)

$$D = 0.02\mu^{-0.3}Fe^{-0.5}(V - V_1)^{1.56} \quad , (V > V_1), \quad (2)$$

where D denotes the sliding displacement, m is the friction coefficient, $V_1 = mg/(2\pi Fe)$ is the minimum velocity needed for sliding. In our estimation, m is assumed to be 0.05 in order to avoid overestimation of the PGV. In addition, considering the predominant frequency of recordings shown in Fig. 2, Fe is varied parametrically as 0.75, 1.5, and 2.25 Hz. Fig. 4 shows the sliding displacement with respect to the PGV for three different values of Fe. It is seen that the displacement D increases as F_e becomes smaller. For most cases in which the soils are not soft, the predominant frequencies are estimated to be greater than 1.5Hz. If a tombstone moved more than 40cm, the PGV is estimated to be more than 90 cm/s. It turns out that PGVs estimated from the toppling ratios or displacements of tombstones are more than 90cm/s in the areas where the wooden house suffered serious damages.

Tabel.2 Summary of damage survey of wooden houses

Town	Name	No. of stories	Const. Year	Roofing*	Damage	Soil. (Hz)	Natural freq. of house	
							Trans.	Long. (Hz)
Yamoto	YYT	2	1993	TL	Slight	5.6	3.8	3.8
	YAM	2	～1900	TL	Slight	7.6	3.5	3.0
	YAS	1	～1800	TH+SS	Slight	10.8	2.7	3.3
	YSH	1	～1850	SS	Slight	6.3	3.2	3.8
	YST	2	1979	TL	Slight	5.8	3.3	3.0
	YIY	1	1904	Tile	Moderate	5.2	2.5	2.1
	YOM	1	～1800	TH+SS	No	4.3	2.0	2.6
Kanan	KST	2	1971	SS	Slight	2.3	3.8	4.7
	KUB	2	1998	TL	Slight	4.8	5.0	4.4
	KII	1	～1840	TH	Minor	-	2.7	2.9
	KUM	1	1950	TL	Minor	3.1	-	-
	KSH	1	1992	TL	Minor	-	5.8	6.8
	KTM	1	1941	TL	Minor	4.7	4.7	3.5
	KKM	2	1945	TL	Moderate	2.0	2.3	2.6
Nango	NNH	2	2000	SL	Slight	0.9	5.5	4.4
	NTK	1	1995	TL	Slight	0.8	4.0	3.7
	NKT	2	1953	TL	Slight	-	-	-
	NSH	1	1950	TL	Minor	0.8	3.9	3.2
	NYM	1	1960	TL	Minor	1.0	3.7	4.0
	NMH	1	～1900	TH+SS	Moderate	0.7	3.5	2.0
	NOH	2	1965	TL	Moderate	-	-	-

* TH:Thatch, TL:Tile, SS:Steel Sheet, SL:Slate

Fig. 5 A typical one-story house house (KII)

Fig.6 Hanging walls (NMH)

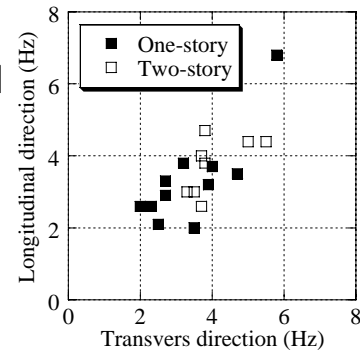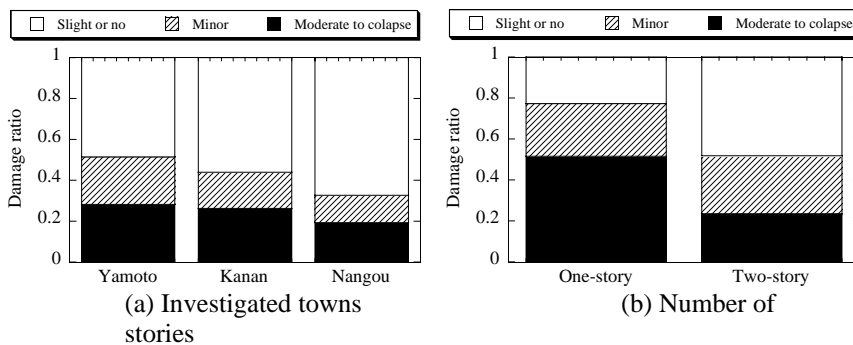(a) Investigated towns stories

(b) Number of

Fig. 8 Fundamental frequencies of one- and two-story houses

5. Evaluation of seismic performance of wooden houses

Structural properties and damages have been investigated for wooden houses in the Yamoto town, Kanan town, and Nango town, where severe damages occurred to many houses. We selected 21 typical houses in the regions without serious damages in order to find why they avoided serious damages under the same strong ground motions. These houses are listed in Table 2. Two different types of roofs were found in the houses. The old houses built 100 years ago are one-story houses or one-story houses partially extended to two stories. Roofing of these houses was originally thatch, but some have changed to tiles or steel sheets. The relatively new houses are covered by steel sheets. Fig. 5 shows a typical one-story house with thatch roofing. Beams in the roof truss were very thick, and consequently the weight of the roof is heavy.

An important feature in the one-story houses is that they usually have hanging walls as shown in Fig. 6,

and the heights of the story and the hanging walls are quite high. The story height ranges from 2.6m to 3.9m, mostly higher than modern houses with heights about 2.7m.

To catch a general trend of the damages, surveys were carried out for houses in the three towns to obtain damage statistics. Fig. 7(a) shows damage ratios of the three towns. As the distance from the epicenter of the main shock increases in the order of the Yamoto town, Kanan town, and Nango town, the damage ratio reduces. The ratio of moderate damage to collapse is about 20% in the Nango town, and about 28% in the Yamoto town. The damage ratio is clearly related to the number of stories, as shown in Fig. 7(b). The ratio of one-story houses with moderate damage to collapse is about 50%, 2.5 times as high as that of two-story houses. While Fig. 7(a) gives an expected trend, the result shown in Fig. 7(b) is surprising, and needs to be investigated.

Fig. 8 shows fundamental frequencies of the wooden houses in the transverse and longitudinal directions. They were obtained from micro-tremor measurements, and therefore, only corresponding to
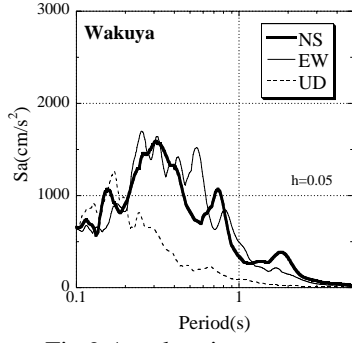
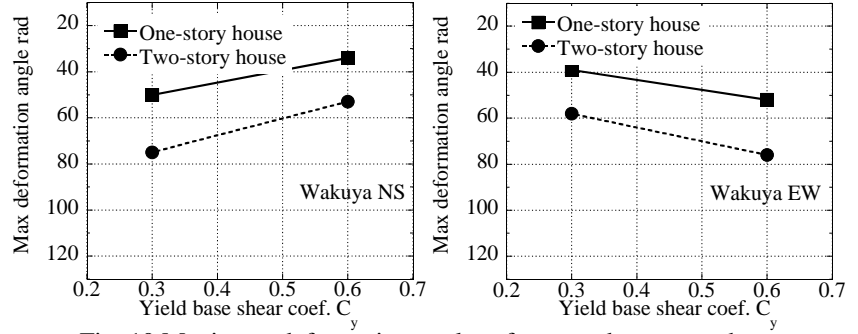Fig.9 Acceleration response
spectra during the main shock

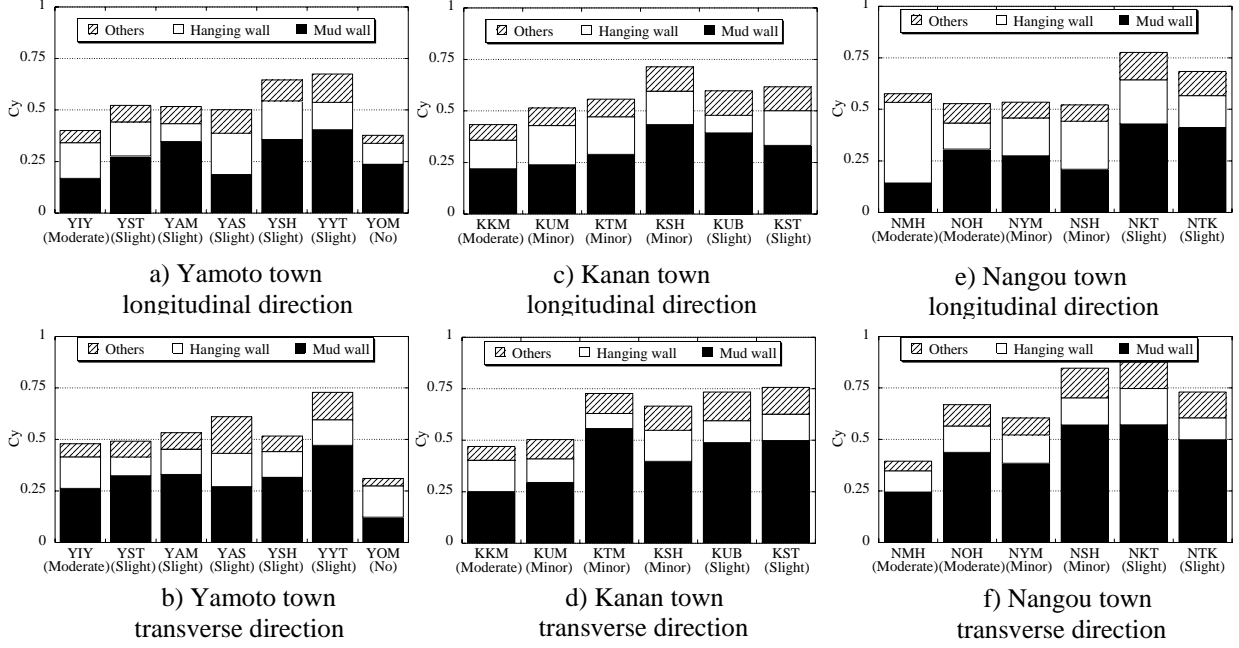Fig. 10 Maximum deformation angles of one- and two-story houses

a) Yamoto town
longitudinal direction

c) Kanan town
longitudinal direction

e) Nangou town
longitudinal direction

b) Yamoto town
transverse direction

d) Kanan town
transverse direction

f) Nangou town
transverse direction

Fig. 11 Yield base shear coefficient

small deformations. The solid and hollow symbols correspond to the one-story and two-story houses, respectively. It is interesting that the fundamental frequencies of the one-story houses are lower than those of two-story houses. This may be due to the differences in roof weights and/or heights of stories, and may be related to the difference in the damage ratios. However, the natural frequencies of wooden houses that are highly nonlinear vary substantially as their deformations increase; thus we would explain the phenomenon in terms of the deformation drift angle.

A method called equivalent-performance response spectrum was developed by Hayashi (2002) to estimate the maximum drift angle based on the knowledge of the ground motion and the wooden house structure. Let a house be modeled by an equivalent SDOF system. An equivalent period T_e for a specified maximum drift angle R is given by

$$T_e = 2\pi \left\{ \left(M_e / M \right) H_e R / C_y g \right\}^{0.5} \quad (3)$$

where Me and He are the effective mass and height of the SDOF system, respectively, and M, Cy, and g are the total mass, yield base shear coefficient, and gravitational acceleration, respectively. For this

SDOF system, an equivalent acceleration response spectrum corresponding to the specified drift angle R is estimated as

$$S_{ae} = Q_y / (M_e F_h) = C_y g / ((M_e / M) F_h) \quad (4)$$

where Fh is the reduction factor of acceleration spectrum depending on the damping ratio h as follows

$$F_h = 1.5 / (1 + 10h)$$

$$h = 0.2 \left\{ 1 - \left(100R \right)^{-0.5} \right\} + 0.05 \quad (5)$$

The maximum drift angle R can then be estimated by equating the equivalent acceleration response spectrum given by Eqs. (3)-(5) to the response spectra of the measured accelerations such as those in Fig. 9. In this study, we assume that Me/M=1.0, He=3.3m for a typical one-story house, and Me/M=0.9, He=5.5m for a typical two-story house, and Cy varies between 0.3 and 0.6. Fig. 10 shows the estimated maximum drift angles corresponding to the recorded ground accelerations at the Wakuya station during the main shock. It is seen that the maximum drift angle of a typical one-story house is larger than that of a typical two-story house. Since the large deformation is the

a) Longitudinal direction
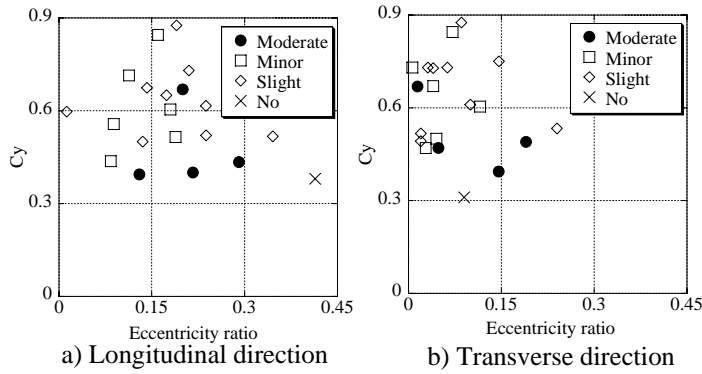
b) Transverse direction

Fig. 12 Yield base shear coefficients and eccentricity ratios of houses

Fig.13 Cracks in hanging wall (YIY)

Fig.14 Separation of lintel-column joint (YIY)

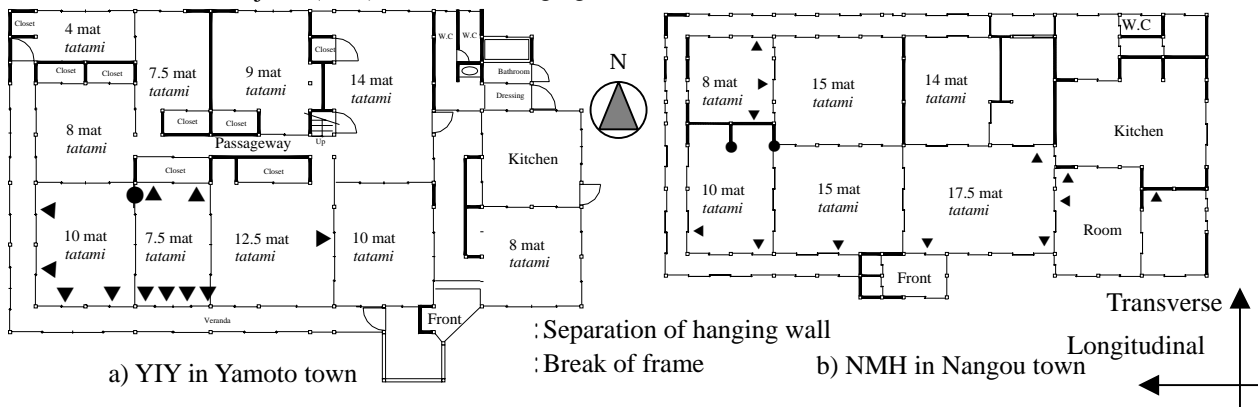Fig.15 separation of hanging wall (NMH)

Fig.16 Break of column (NMH)

a) YIY in Yamoto town

Separation of hanging wall
Break of frame

b) NMH in Nangou town

Transverse
Longitudinal

Fig.17 Ground plans of houses

direct cause of the damages, the maximum drift angles R less than 1/30rad correspond to a low ratio of severe damages at the location. This result is consistent with the statistics shown in Fig. 7(b).

To evaluate the seismic performance of the 21 selected houses, the response limit strength design method has also been applied. It has been modified by Suzuki et. al. (2003) to be suitable for wooden houses. As one of the major modifications, several unit structural elements are identified for wooden houses, and their force-displacement relationships are determined by tests. These elements are then integrated to constitute a specific wooden house, and its force-displacement curve is calculated analytically based on those of the elements.

Applying the response limit strength design method, we have calculated contributions of different structural elements toward the yield base shear coefficient C_y. Since C_y is defined at the deformation angle of 1/30rad that is considered to be a typical yield point, it reflects the strength of the structure. In

general, C_y ranges from 0.4 to 0.8 in both the longitudinal direction and transverse direction. Fig. 11 shows the contributions of three different structural elements to C_y for the 21 houses in two directions. One third to half of the total yield shear is loaded to mud walls, and another one third to half is loaded to hanging walls. Thus, the hanging walls play very important role in the seismic performance.

Besides the strength represented by the yield base shear coefficient C_y, the structural asymmetry of the houses may be also an important factor for the damages. Fig. 12 shows both the C_y and eccentricity ratio of the first story in the transverse and longitudinal direction, respectively, for the selected wooden houses. In calculating the eccentricity ratio, the center of gravity of a wooden house was determined by taking the maldistribution of the 2-story into consideration. Although not very clear, Fig. 12 does give a general trend that a wooden house with a large eccentricity ratio and a low yield base shear coefficient is more likely to be damaged during

earthquakes.

Among the four houses with moderate damages, the YIY and NMH houses had frame damage. In both houses, frame damages occurred at the lower joint of lintels and columns. Since frame damages are crucial for a wooden house, these two houses need to be investigated in more details.

Fig. 13 shows cracks in a hanging wall in YIY house, while Fig. 14 shows the separation of a lintel from its connecting column. Since site conditions of the seven houses in the Yamoto town are similar, differences in damage level are mainly due to the differences in their seismic performance. This is substantiated by the analytical results shown in Fig. 11(a), that the strength of the YIY house is the second lowest in the Yamoto town in the longitudinal direction. Fig. 17(a) shows the ground plan of the YIY house, where most cracks in the hanging walls and the damage in a lintel-column joint were observed in the longitudinal direction. The damages were concentrated in the southwest part of the house due to the eccentricity and also indicated insufficient walls in this part.

For the NMH house, the separation of the hanging walls and the break of a column are shown in Figs. 15 and 16, respectively. The damages can also explained by the weak seismic performance of the structure. The strength of the NMH house in the transverse direction is the lowest in the Nangou town, as shown in Fig. 11(f), and about 70% of the total strength in the longitudinal direction was provided by hanging walls, as shown in Fig. 11(e). The ground plan of the NMH house is shown in Fig. 17(b), where most of damages took place in the south part and west part due to the asymmetry of the house.

The damages at the joints of the hanging walls (lintels) and the columns in both YIY and NMH houses point out that the over concentration of the strength in the hanging walls may be a reason for the frame damages.

In applying the method of response limit strength design, the force-deformation curve for the hanging wall was obtained from test specimens in the lab. However, the heights of the hanging walls in the 21 houses are much larger than that used in the tests. Thus, the shear failure shown in Fig. 6 will not occur in the lab. To improve the method for evaluating the seismic performance of existing buildings, the force-deformation relationship of the unit elements should be obtained through tests on real scale specimens.

6. Conclusions

Damages of wooden houses during the Northern Miyagi earthquakes have been investigated. First, earthquake observation records are summarized. The PGVs in the areas where the wooden house suffered serious damages are estimated based on the toppling ratios or displacements of tombstones. Surveys were conducted in three towns to obtain statistics of the damages. It is found unexpectedly that the damage ratios of one-story houses are much higher than those of two-story houses in all three towns. This damage trend is analyzed and explained by using the method of equivalent performance response spectrum. Two factors are found to be critical for the seismic performance of a house: one is its strength, and another is its eccentricity. To determine the strength, the response limit strength design method is employed. It is found that a wooden house with a large eccentricity ratio and a low yield base shear coefficient is vulnerable during earthquakes. Two houses with frame damages are investigated in more details. It is found that while high hanging walls contribute considerably to the total strength, the joints of the hanging wall and the columns may be damaged due to the over concentration of the strength.

References
1) Kaneko, M. and Y. Hayashi (2000) : Proposal of a Curve to Describe Overturning Ratios of Rigid Boies, *AIJ*, No. 536. pp.55-62 (in Japanese).
2) Kaneko, M., Y. Hayashi, and K. Tamura : Evaluation of Sliding Displacement of Furniture during Earthquake -By using Revised Formula to Estimate Sliding Displacement of Furniture, *Trans. of AIJ*, B-2, pp.527-528, 1999 (in Japanese).
3) Hayashi, Y, :Evaluation of Seismic Design Load based on Equivalent-Performance Response Spectra, Proc. of 11th JEES, pp. 651-656, 2002.11 (in Japanese).
4) Suzuki Y., Y. Saito, K. Katagihara, K. Ikago, and C. Nojima: Method of Evaluating Seismic Performance of Wooden Frames - Limit Bearing Capacity Analysis in Wide Range of Deformation -, Proc. of 11th JEES, pp.1523-1528, 2002.11 (in Japanese).
5) *AIJ*, Damege survey in northern Miyagi, Japan, earthquakes of July 26, 2003 preliminary report, 2003.8 (in Japanese).
6) http://www.kik.bosai.go.jp/kik/index_en.shtml
7) http://www.k-net.bosai.go.jp/
8) http://www.nilim.go.jp/japanese/database/nwdb/

2003

90cm/s

:   ,

COE31.

2003年7月26日宮城県北部の地震における被災木造建物の耐震性能評価

○　清水秀丸・鈴木祥之・林康裕

1．はじめに

2003年7月26日、宮城県北部で発生した一連の地震では、多くの木造建物が被災した。被害の大きかった地域の被災木造建物の構造詳細調査を行った結果、算出される耐震性能評価について報告する。また、耐震性能評価と地震被害との整合性についての分析も実施する。

2．調査建物概要

軸組構法木造建物を対象とした、構造詳細調査を、矢本町小松地区、河南町北村地区、南郷町二郷地区で実施した。築200年以上から築3年までの平屋、2階建てを各地区で7棟ずつ、計21棟の詳細調査より、平面図、耐震要素の抽出、重量算定などを行い、構造的特徴を把握した。矢本町の調査建物一覧を表1に示す。

この地域の構造的特徴として、写真1に示すような、平屋建物が多く、調査した建物中、12棟が平屋建てであった。また、写真2のように、階高が高く、小壁高さも高い建物が多く見られ、この地域では、小壁は重要な耐震要素と考えられる。

3．被災建物の耐震性能評価

対象建物の詳細調査に基づき、土壁、土壁小壁、石膏ボード、石膏ボード小壁、貫、柱ほぞを耐震要素として各建物の復元力特性を算出した。算出方法は各耐震要素の耐力を加算する限界耐力計算の手法を用いて算定した。

限界耐力計算を木造に適応する手法では、隣接する全面壁が無い場合、小壁は層間変形角1/30radで柱の鴨居部分に生じる曲げにより柱の折損を主体とした破壊モードによって耐震性能を失うと仮定されているが、調査建物では柱の折損を確認することが出来なかった。また詳細調査結果より、小壁はせん断による破壊モードが発生したと考えられるため、本論文において小壁は1/15radまでの耐力と変形性能を有すると仮定した。

建物重量の算出については調査時に各建物の小屋裏の調査がほとんどの建物で可能だったため、屋根材、小屋裏に配置されていた土壁なども算出した。茅葺き、壁の重量は、重要文化財(建造物)耐震診断指針及び建築基準法に基づき、床面積当たりの単位重量より算出した。

1/30rad時のベースシア係数Cにおける矢本町、桁行き方向の各耐震要素負担率C_yを図1に示す。地震被害との整合性では、無被害のYOM邸が最も低いC_yを示した。しかし、7棟すべての結果より、被害程度と耐震性能評価結果は、良い対応関係が見られた。また、小壁は耐震要素として有効であり、C_yに占める割合が大きいことを確認した。

4．まとめ

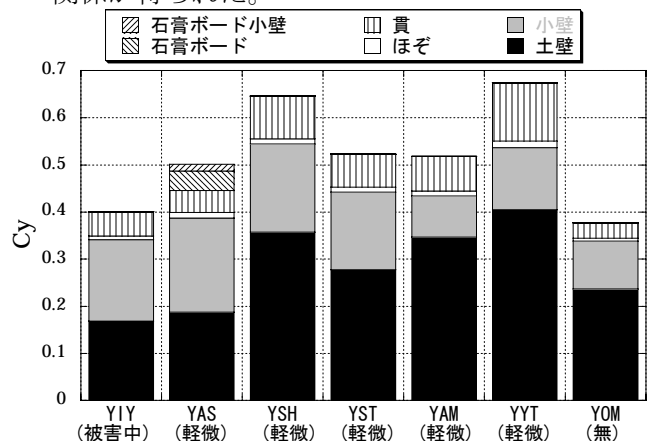宮城県北部地震の被災木造建物を対象として限界耐力計算法に基づいて、耐震性能評価を実施した。被害程度と耐震性能評価結果は、良い対応関係が得られた。

図1　桁行き方向の耐力負担割合

表1　矢本町詳細調査建物一覧

	建物名	階数	建築年	屋根材	被災度
矢本町	YIY	平屋	1904	瓦	中
	YAS	平屋	～1800	鉄板	軽微
	YSH	平屋	～1850	鉄板+瓦	軽微
	YST	2階	1979	瓦	軽微
	YAM	部分2階	～1900	瓦	軽微
	YYT	2階	1993	瓦	軽微
	YOM	平屋	～1800	茅葺+鉄板	無

写真1　平屋建物の一例

写真2　小壁の概要